Available online at www.sciencedirect.com
SCIENCE DIRECT®
ELSEVIER
Polymer 47 (2006) 3344–3350
polymer
www.elsevier.com/locate/polymer

Palygorskite as an epoxy polymer reinforcement agent

Siqi Xue [a], Marc Reinholdt [b], Thomas J. Pinnavaia [a,*]

[a] *Department of Chemistry, Michigan State University, 320 Chemistry Bldg., East Lansing, MI 48824, USA*
[b] *Department of Geology, University of Illinois at Urbana-Champaign, Urbana, IL 61801, USA*

Received 8 January 2006; received in revised form 7 March 2006; accepted 8 March 2006

Abstract

Palygorskite, a silicate clay with a pleated 2:1 layered structure, has a lath-like particle morphology that makes it an attractive candidate for the formation of polymer nanocomposites. Here, we report the properties of palygorskite in pristine and silylated forms for the reinforcement of rubbery and glassy epoxy matrices. Three silylation reagents were used for surface modification of the mineral, namely, γ-aminopropyltrimethoxysilane (APTMS), *N*-dodecyltriethoxysilane (DTES), and 1,1,1,3,3,3-hexamethyldisilazane (HMSZ). The silylated palygorskite derivatives provided better dispersions in rubbery epoxy matrices than the pristine mineral, affording improvements in mechanical properties at low loadings levels of 2 and 5% (w/w). But at higher loadings where increases in the viscosity of the pre-polymer helps to stabilizes the mineral dispersion, little or no differences were observed for the reinforcement benefits provided by the pristine and silylated forms of palygorskite. Glassy epoxy nanocomposites formed from both pristine and silylated palygorskite exhibited marginal improvements in tensile properties regardless of the mineral loading level, suggesting that the tensile strength of the pleated sheet silicate may be approaching that of the polymer matrix.

Keywords: Palygorskite; Epoxy; Nanocomposites

1. Introduction

Montmorillonite and other members of the smectite family of clay minerals have been extensively studied as polymer reinforcement agents [1–4]. In order to make these intrinsically hydrophilic clays compatible with polymer matrices, onium–ion exchange reactions normally are used to mediate the surface polarity. When the organoclay derivatives are dispersed as individual 1-nm thick sheets in a polymer matrix, resulting nanocomposites usually exhibit excellent mechanical properties, thermo-stability, barrier property, fire retardant, and other material properties.

Palygorskite and sepiolite have structures related to the 2:1 layered structure of smectite clays, except that the layers are pleated to form cross-linked ribbons [5,6]. This cross-linking feature precludes the possibility of exfoliating the structure into 1-nm thick nanoparticles. Nevertheless, owing to the relatively high surface area and lath morphology of these minerals, particularly in the case of palygorskite, they have found use as absorbents, pigments, catalysts, and rheological control agents [5,7–10]. However, palygorskite has received relatively little attention as a polymer reinforcement agent with only a few studies being devoted to composites of polyolefins, polyurethane, polyimide, and polyamide [11–19].

In the present work, we investigate the properties of pristine and silylated palygorskite for the reinforcement of rubbery and glassy epoxy polymers. Silylation has been used previously to modify the surface polarity of palygorskite [20], as well as other mineral [21–23] and synthetic silicates [24] with potential polymer reinforcement properties. Silylation also is used in the present work to enhance the hydrophobic character of palygorskite and to improve its dispersion in an epoxy matrix.

2. Experimental

2.1. Materials

The commercially available diglycidyl ethers of bisphenol A (DGEBA) with the structure shown in Scheme 1 were provided by the Shell company under the trade names Epon

---

* Corresponding author. Tel.: +1 517 432 1222; fax: +1 517 432 1225.
E-mail address: pinnavaia@chemistry.msu.edu (T.J. Pinnavaia).

0032-3861/$ - see front matter © 2006 Elsevier Ltd. All rights reserved.
doi:10.1016/j.polymer.2006.03.036

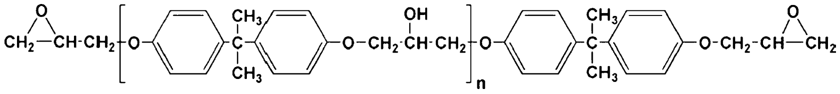

Scheme 1. Epon epoxy resins.

828 [$n=0$ (88%), 1 (10%), 2 (2%)] and Epon 826 [$n=0$ (99%), $n=1$ (1%)].

The curing agents, shown in Scheme 2, were α,ω-polyoxypropylene diamines provided by Huntsman Chemicals under the trade names Jeffamine D2000 [$x=33.2$, MW ~ 2000] and Jeffamine D230 [$x=2.6$, MW ~ 230] or the glassy system, respectively (Scheme 2).

Palygorskite was provided by the Active Minerals Company LLC under the trade name Acti-Gel 208. Other chemicals were purchased from Aldrich Chemical Co. and were used as received.

2.2. Palygorskite purification

The as-received palygorskite was found to contain small amounts of mineral impurities. A purification process was carried out by preparing a 10 wt% aqueous suspension of the mineral and allowing the more dense impurities (quartz and carbonates) to sediment out. After a certain sedimentation time, the supernatant suspension was decanted off and the sedimentation process continued. X-ray diffraction analysis of each sediment fraction provided an indication of the purity of the mineral remaining in suspension. The purification was repeated until there was no evidence by X-ray diffraction for the presence of quartz or carbonate minerals in the sediment. The purified mineral remaining in suspension then was collected and used to form nanocomposites for comparison with composites made from as-received palygorskite. Survey experiments revealed no difference in the mechanical properties of epoxy composites prepared from the purified and as-received palygorskite. Accordingly, for use in all subsequent experiments, the as-received palygorskite was dispersed in acetone and subjected to sonification for 30 min. The suspension was evaporated in air to collect the mineral.

2.3. Palygorskite silylation

The silylation of palygorskite was carried out in a mixture of the clay and the silylation reagent in toluene under reflux conditions. Prior to silylation reaction, the mineral was oven dried at 120 °C for 2 h to remove water from the external surfaces. A 1- to 2-g amount of palygorskite and a stoichiometric amount of silylation agent were added to 50 mL of toluene. The amounts of silylation agent used were determined by assuming there were four silanol sites per square nanometer of clay surface area. The mixture was submitted to ultrasonication for 30 min and then the suspension was heated under reflux for 4 h. The resulting silylated product was air-dried, ground in a mortar and pestle, and used for nanocomposite formation. The silylation reagents used were γ-aminopropyltrimethoxysilane (APTMS), *N*-dodecyltriethoxysilane (DTES), and 1,1,1,3,3,3-hexamethyldisilazane (HMSZ). The corresponding silylated palygorskite (PLG) clays were denoted APTMS–PLG, DTES–PLG, and HMSZ–PLG, respectively.

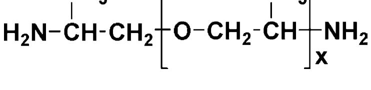

$$H_2N-\overset{CH_3}{CH}-CH_2\left[O-CH_2-\overset{CH_3}{CH}\right]_x NH_2$$

Scheme 2. Jeffamine α,ω-polyoxypropylene diamines.

2.4. Composites preparation

Both as-received and silylated palygorskite materials were used to make rubbery or glassy epoxy composites. Equivalent amounts of epoxy monomer and curing agent were mixed at 75 °C for 10 min, out-gassed at room temperature for 20 min, and transferred into a dog-bone shaped aluminum mold for curing. The composites were partially cured at 75 °C for 3 h and then fully cured at 125 °C for 3 h under nitrogen flow.

2.5. Characterization methods

X-ray diffraction (XRD) patterns were obtained on a Rigaku rotaflex 200B diffractometer equipped with Cu Kα X-ray radiation and a curved crystal graphite monochromator, operating at 45 kV and 100 mA. Clay films for X-ray diffraction analysis were prepared by dripping droplets of aqueous clay suspension onto a glass slide and allowing the suspensions to dry. The diffraction patterns were recorded from 1 to 70° 2θ with a step scan of 0.02°/point and a scan rate of 0.5°/min. Cured composite samples were prepared by fitting rectangular flat specimens into the windows of aluminium holders. The patterns were recorded from 1 to 40° 2θ with a step interval of 0.05°/point and a scan rate of 2°/min.

TEM images were obtained on a JEOL 2010F 200 kV field emission TEM with an acceleration voltage of 200 kV. The clay samples for TEM imaging were prepared by evaporating clay–ethanol suspensions on a holy carbon coated copper grid. Composites samples for TEM imaging are in the form of 80–100 nm thick thin-sections supported on a copper grid.

The tensile measurements on dog-bone shaped samples were carried out at room temperature according to ASTM procedure D3039 using an SFM-20 United Testing System equipped with a laser extensometer. The measurements were conducted with a crosshead speed of 25 mm/min for rubbery samples and 0.5 mm/min for glassy samples. The reported tensile parameters are values averaged over four independent specimens.

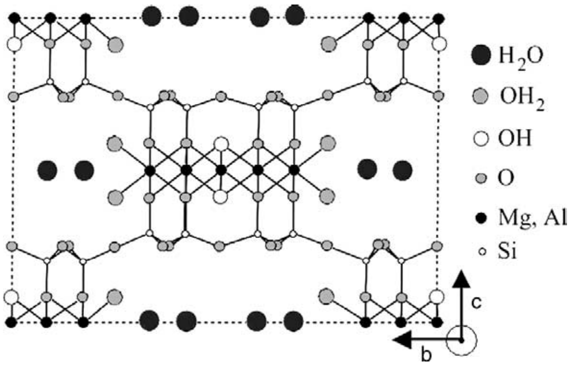

Fig. 1. A schematic [100] projection of palygorskite structure [6].

FTIR spectra of samples dispersed in KBr disks were recorded at ambient temperature on a Mattson Galaxy 3000 FTIR spectrometer over the range 400–4000 cm^{-1}. ^{29}Si MAS NMR spectra were obtained at 79.4 MHz on a Varian VXR-400S solid state NMR spectrometer equipped with a magic angle spinning probe. For each measurement the sample was spun at 4 kHz. The pulse delay was 400 s, and chemical shifts were referenced to talc. Thermogravimetric analyses (TGA) were carried out on a Cahn TG System 121 Analyser. The powdered clay samples were heated to 800 °C at a rate of 5 °C/min.

3. Results

3.1. Characterization and purification of palygorskite

Palygorskite, with an idealized unit cell formula of $M^{2+}_{(x+y+2z)/2} \cdot nH_2O[Mg_{5-y-z}R_y\square_z](Si_{8-x}R_x)O_{20}(OH)_2(H_2O)_4$, where R is Al (III) or Fe (III), □ is an interstitial vacancy, and M^{2+} is an exchangeable cation, adopts the pleated layered structure shown in Fig. 1 [6,25]. The linked ribbons represent a 2:1 layer that is continuous along the *a*-axis, but of limited lateral extend along the *b*-axis. Rectangular channels, formed through the pleating of sheets, contain exchangeable Ca^{2+} and Mg^{2+} cations, zeolitic water, and water molecules bound to coordinatively unsaturated metal ion centers at the edges of the ribbons. Small polar molecules, such as ammonia, and acetone, can access the tunnels by displacing the zeolitic water molecules upon partial dehydration of the clay materials. Further dehydration enables the formation of bonds between terminal Mg (II) and the small molecules to afford hybrid materials [26,27].

Sedimentation of a 10% (w/w) aqueous suspension of the mineral was used to separate the clay from quartz and carbonate impurity phases [8]. Fig. 2 shows the X-ray patterns of the sedimented fractions collected after different settling times. The impurity phases were almost completely removed from the suspension after an aging time of 14 days. Owing to the low concentrations of the impurity phases, composites made from the as-received and purified versions of the mineral showed no difference in mechanical properties. Thus, the as-received mineral was used in all nanocomposite experiments.

Nitrogen adsorption measurements indicated the total BET surface area of the as-received palygorskite to be 182 m^2/g (65% external surface area), which is substantially larger than the surface area for pristine montmorillonite (∼7 m^2/g, 100% external surface area). The TEM images provided in Fig. 3 clearly show the presence of bundled lath-like crystals of palygorskite ∼5 to 20 nm in width and several micrometer in length. Thermal gravimetric analysis showed the loss of water over three temperature regions corresponding to the loss of 7.5% (w/w) surface and zeolitic water at 25–130 °C, 3% coordinated water (130–270 °C), and 6.5% water due to dehydroxylation of the 2:1 layered structure (>270 °C) [10]. The ^{29}Si MAS NMR spectrum of the as-received palygorskite (not shown) contains two Q^3 peaks at −98 and −92 ppm, corresponding to SiO_4 units at the central and edge positions of the ribbons, respectively [9]. The absence of a resonance characteristic of SiOH groups (∼ −84 ppm), indicates that the fraction of silicon centers at the external surfaces of the laths is very small (<2%).

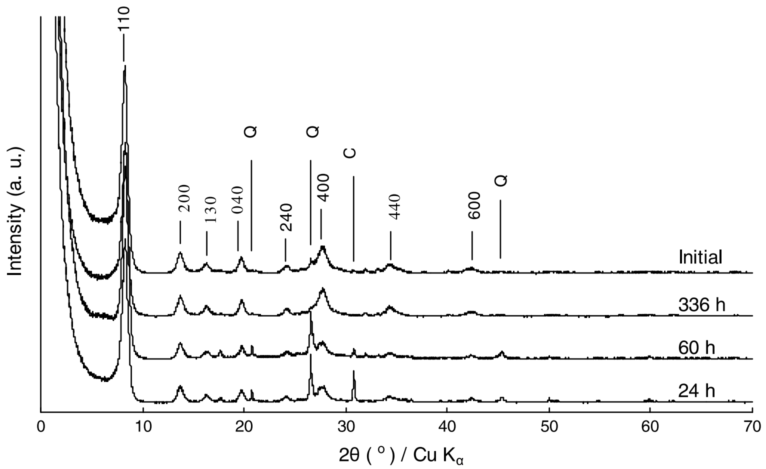

Fig. 2. The *hkl* X-ray reflections of as-received palygorskite and of the sedimented fractions obtained upon aging a 10% (w/w) aqueous slurry of the mineral. Q and C mark diffraction peaks indicative of quartz and carbonate mineral impurities, respectively.

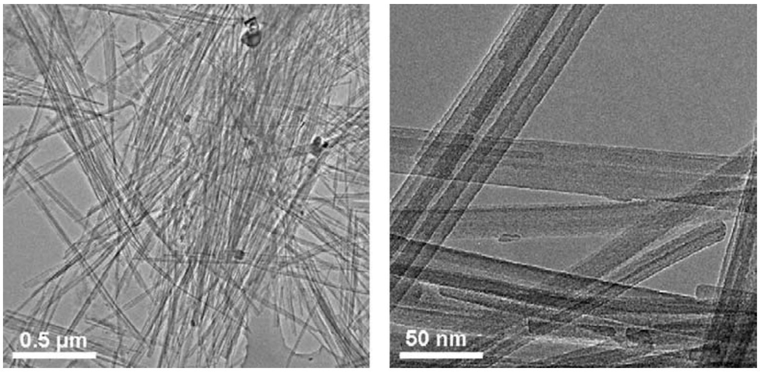

Fig. 3. TEM images of as-received palygorskite.

3.2. Silylated palygorskite

The silylation reactions of palygorskite with γ-aminopropyltrimethoxysilane (APTMS), *N*-dodecyltriethoxysilane (DTES), and 1,1,1,3,3,3-hexamethyldisilazane (HMSZ) resulted in no changes in the XRD pattern or the ^{29}Si MAS NMR spectrum of palygorskite. The N_2 adsorption–desorption isotherms show that the BET surface area of the HMSZ silylation product, denoted HMSZ–PLG, was 122 m^2/g, slightly reduced from the 182 m^2/g surface area of the pristine material. The FTIR spectra of the as-received palygorskite and the HMSZ–PLG silylation product are compared in Fig. 4. Weak C–H stretching vibrations near 2900 cm^{-1} are observed for HMSZ–PLG, indicating that trimethylsilyl groups have been coupled to the external surfaces of the mineral. Analogous FTIR bands were observed for the APTMS- and DTES-PLG reaction products. Additional evidence in favor of silylation was provided by the inability of the silylation products to disperse in water. The degree of silylation was $<2\%$ (w/w), as judged by TGA measurement.

3.3. Epoxy nanocomposites

Rubbery and glassy epoxy nanocomposites were prepared by dispersing as-received and silylated forms of palygorskite in degassed equivalent amounts of epoxy monomer and curing agent and then curing the mixtures under nitrogen. The dispersion of the mineral was qualitatively judged by examining the relative intensities of palygorskite diffraction peaks obtained from the bottom and top surfaces of the composite specimens. As seen by the comparison of 110 and 400 reflections in Fig. 5, much more palygorskite settles to the bottom of the composite made from as-received palygorskite in comparison to the silylated palygorskite composite. The top surfaces of both specimens show no palygorskite reflections, indicating that there is a graded distribution of palygorskite from top to bottom in both cases. But the particle gradient is substantially less for the composite made from silylated palygorskite than for as-received palygorskite.

A TEM image of a thin-section of a glassy epoxy composite containing 5% (w/w) HMSZ–PLG is shown in Fig. 6. In comparison to the image for the pristine clay in Fig. 3, the clay

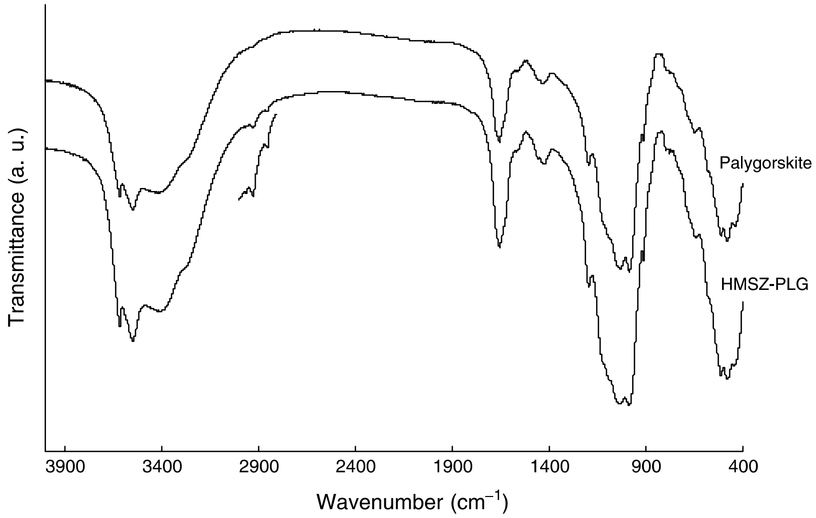

Fig. 4. FTIR spectra (KBr) of as-received palygorskite and the HMSZ silylation product. The inset shows an expansion of the C–H stretching region between 2800 and 3000 cm^{-1} for HMSZ-palygorskite.

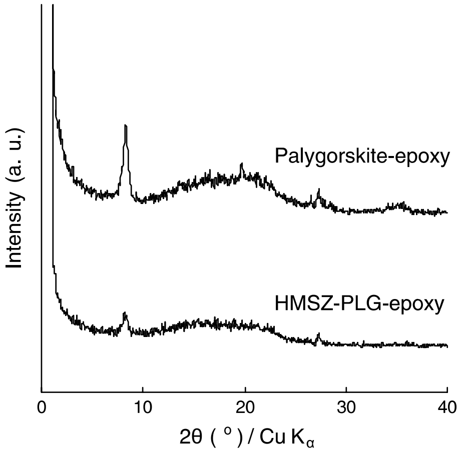

Fig. 5. XRD patterns of the bottom sides of epoxy nanocomposite specimens prepared from as-received and silylated palygorskite.

laths in the composite appear to be thinner, suggesting that the aggregation of clay laths is reduced in the composite.

Representative stress–strain curves for HMSZ–PLG reinforced rubbery epoxy composites are presented in Fig. 7. The mechanical properties of rubbery and glassy epoxy composites containing 0–10% (w/w) palygorskite are given in Tables 1 and 2, respectively. Included in Table 1 for comparison are the tensile properties of a rubbery epoxy nanocomposite reinforced by an organo-montmorillonite [28]. The tensile properties of the rubbery composites are substantially improved in comparison to the pristine polymer, but less so for the glassy composites.

4. Discussion

The commercial form of palygorskite used in this study contained detectable amounts of quartz and carbonate minerals (cf. Fig. 2). However, these impurity phases were present in such small amounts that their removal by sedimentation methods did not improve the nanocomposite performance properties of the mineral. The hydrophilic nature of pristine palygorskite arises from the presence of coordinated water at the edges of the pleated 2:1 layers and the filling of the channels by zeolitic water (cf. Fig. 1). Thermal dehydration of the mineral removes the channel water, but dehydration is not expected to alter the hydrophilic nature of the laths, because terminal hydroxyl groups still decorate the external edge and base surfaces of the structure. Thus, pristine palygorskite was not effectively dispersed in the epoxy pre-polymer and tended to sediment out prior to polymer curing. However, silylation of the mineral substantially improved dispersion, even though a graded distribution of particles was evident based on the presence of observable XRD reflections from the bottom surfaces of a specimen containing 5% (w/w) of the mineral (cf. Fig. 5).

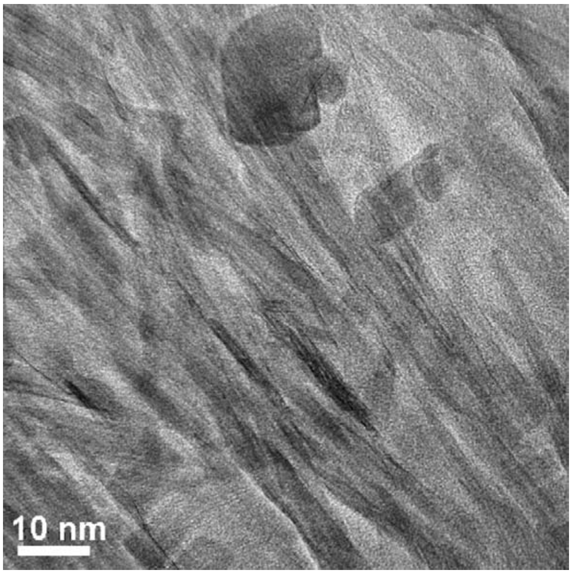

Fig. 6. TEM image of a thin-section of a glassy epoxy nanocomposite containing 5% (w/w) of HMSZ–PLG.

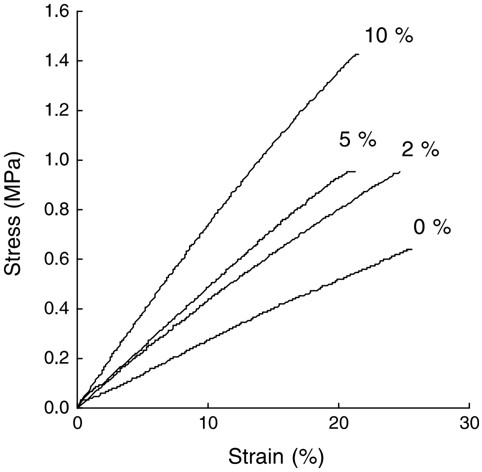

Fig. 7. Representative strain–stress curves for rubbery epoxy composites containing different loadings of silylated palygorskite HMSZ–PLG.

The silylation of palygorskite was readily accomplished using γ-aminopropyltrimethoxysilane (APTMS), *N*-dodecyltriethoxysilane (DTES), and 1,1,1,3,3,3-hexamethyldisilazane (HMSZ) as silylating agents. The presence of silylated surfaces was verified by FTIR (cf. Fig. 4). Bands near 2900 cm^{-1} were assigned to C–H bond stretching modes of the grafted organosilane, in accord with previous assignments [22–24]. It is noteworthy that the broad bands at 3556 cm^{-1} due to coordinated water and at 3410 and 3283 cm^{-1} due to zeolitic water [7] indicated the retention of the channel water after silylation in toluene under reflux conditions. The sharp band at 3620 cm^{-1} is assigned to the stretching mode of hydroxyl groups in the 2:1 ribbons. Thus, the silylation of the mineral was confined to hydroxyl groups at the external edge and basal surfaces. The hydrophobic nature of the silylated products was evidenced in part by the inability to suspend the products in water.

The comparison of tensile properties in Table 1 for a rubbery epoxy matrix shows that as-received palygorskite provides some improvement in the modulus, but little or no

Table 1
The tensile properties of rubbery palygorskite–epoxy composites

Nanoparticle and nanoparticle loading (%)	Tensile strength (Mpa)	Tensile modulus (Mpa)	Tensile elongation (%)
None	0.62 (6.8%)	2.8 (5.0%)	25.0 (8.0%)
Palygorskite			
2	0.71 (8.2%)	4.4 (7.7%)	25.3 (9.2%)
5	0.74 (8.5%)	4.0 (6.9%)	20.7 (8.9%)
10	1.32 (7.3%)	5.0 (6.4%)	28.1 (9.0%)
APTMS–PLG			
2	0.81 (4.7%)	4.7 (7.0%)	24.0 (10.3%)
5	0.89 (5.5%)	3.5 (6.0%)	28.4 (8.8%)
10	1.03 (9.2%)	4.4 (7.3%)	21.8 (9.8%)
DTES–PLG			
2	1.18 (2.3%)	4.7 (5.2%)	30.9 (2.6%)
5	0.98 (4.2%)	3.5 (9.1%)	30.8 (5.5%)
10	1.47 (6.3%)	6.2 (8.4%)	26.0 (7.7%)
HMSZ–PLG			
2	0.97 (5.0%)	4.8 (3.8%)	24.3 (8.1%)
5	1.00 (7.2%)	5.4 (6.0%)	21.1 (6.0%)
10	1.35 (6.4%)	6.7 (9.5%)	21.2 (13.4%)
$CH_3(CH_2)_{17}NH_3^+$– montmorillonite–epoxy [28]			
0	~0.5	~2.6	–
2	~0.8	~5.5	–
5	~1.5	~7.5	–
10	~3.3	~13	–

Numbers in the parentheses are relative standard deviations.

improvement in the tensile strength at loadings of 2 and 5% (w/w). The abrupt increase in tensile strength at a loading of 10% (w/w) is associated with an increase in the viscosity of the pre-polymer–palygorskite mixture. The increase in viscosity retards the settling-out of the as-received mineral prior to curing and provides a more uniform dispersion of palygorskite particles in the matrix. In comparison to the pristine mineral, the silylated mineral improves the degree of dispersion at loadings of 2 and 5% (w/w). Consequently, improved tensile properties are observed at these lower loadings for the silylated mineral. But at a loading level of 10% (w/w), where the increased viscosity of the pre-polymer facilitates the dispersion of the pristine mineral, there is little difference in the tensile properties of the composites formed from as-received and silylated palygorskite.

It is remarkable that the pristine mineral in the absence of any organic modifiers provides approximately a twofold increase in strength and modulus for the rubbery epoxy matrix at 10% loading. Other pristine clay minerals (e.g. montmorillonite) invariably weaken an engineering polymer, regardless of the level of loading. The low layer charge, lath-like morphology and high surface area (182 m^2/g) of palygorskite makes it much more suitable for polymer reinforcement in comparison to pristine smectite clays, which retain their low surface area tactoidal form ($<10\ m^2/g$) when dispersed in a polymer matrix.

In general, the as-received and silylated forms of palygorskite all provide a substantial benefit in tensile properties at a loading of 10% (w/w), or 5.4% (v/v), due in large part to the improved dispersion of the mineral laths in the matrix (cf. Table 1). However, as shown in Table 1 for $[CH_3(CH_2)_{17}NH_3]^+$exchanged montmorillonite [28], this organoclay provides ~5 to 6 fold increases in tensile properties at a loading of 10% (w/w), or 8% (w/w) on a silicate base. In comparison, palygorskite at the same loading level provides only 2 to 3 fold improvements in tensile properties. Nevertheless, it also must be realized that the improvements achieved with palygorskite come at a level of organic modification that is <0.2% of the levels needed to achieve the dispersion of montmorillonite in the polymer matrix. Thus, the benefit to cost ratio lies in favor of palygorskite.

Despite the reinforcement achieved for a rubbery epoxy matrix, little or no benefit is realized when silylated palygorskite is dispersed in a glassy matrix (cf. Table 2). In view of the pleated layer structure of palygorskite, the tensile properties of the mineral may be approaching those of the polymer matrix itself, thus precluding the possibility of

Table 2
Tensile properties of glassy epoxy reinforced by silylated palygorskite HMSZ–PLG

Clay loading (wt%)	Tensile strength (MPa)	Tensile modulus (GPa)	Tensile elongation (%)
0%	66.1 (1.4%)	2.9 (7.0%)	3.9 (4.0%)
2%	67.1 (2.1%)	3.1 (8.7%)	3.6 (4.6%)
5%	66.0 (2.5%)	3.0 (3.2%)	3.9 (2.8%)
10%	68.9 (4.0%)	3.3 (5.3%)	3.5 (6.1%)

Numbers in the parentheses are relative standard deviations.

reinforcement. Further studies are needed to explore this possibility.

Although palygorskite has been investigated as a reinforcement agent for several other polymer systems [11–19], the benefits seldom approach those observed for the soft polymer matrix standard in the present work. For instance, the tensile strength of polyethylene–palygorskite formed by in-situ polymerization was increased by a maximum of only 20% in comparison to the pristine polymer [15,16,19]. For the related polypropylene–palygorskite composite system, the clay served as a good nucleating agent for isotactic polypropylene, and the relative crystallinity and crystallization temperature of the composite materials generally increased with filler content [17]. An improvement of only 25% in mechanical properties was found for polyimide composites containing 5% palygorskite [13].

Among the best improvements previously reported for any palygorskite composite was the 220% boost in tensile strength found for polyurethane reinforced by 10% (w/w) of the mineral silylated by *N*-[3-(trimethoxysilyl)propyl]ethylenediamine [14]. As note above, comparable levels of reinforcement are obtained for the rubbery epoxy composites reported in the present work, even without silylation of the mineral. Thus, the key to achieving polymer reinforcement benefits with palygorskite lies first in achieving optimal particulate dispersion, whether the dispersions are achieved through viscosity increases in the pre-polymer or through surface modification of the mineral itself.

Acknowledgements

This work has been supported in part by NASA and by the Active Minerals Company, LLC. S.X. acknowledges fellowship support by the Taita Chemical Co.

References

[1] Becker O, Simon GP. Adv Polym Sci 2005;179:29–82.
[2] D'Souza NA. Encyclopedia of nanoscience and nanotechnology, vol. 3; 2004, American Scientific Publishers [p. 253–65].
[3] Okamoto M. Encyclopedia of nanoscience and nanotechnology, vol. 8; 2004, American Scientific Publishers [p. 791–843].
[4] Ray SS, Okamoto M. Prog Polym Sci 2003;28(11):1539–641.
[5] Murray HH. Appl Clay Sci 2000;17(5–6):207–21.
[6] US geological survey open-file report 01-041: http://pubs.usgs.gov/of/of01-041/htmldocs/clays/seppaly.htm.
[7] Augsburger MS, Strasser E, Perino E, Mercader RC, Pedregosa JC. J Phys Chem Solids 1998;59(2):175–80.
[8] Chipera SJ, Bish DL. Clays Clay Miner 2001;49(5):398–409.
[9] D'Espinose de la Caillerie J-B, Fripiat JJ. Clay Miner 1994;29(3):313–8.
[10] Guggenheim S, van Groos AFK. Clays Clay Miner 2001;49(5):433–43.
[11] Shen L, Lin Y, Du Q, Zhong W, Yang Y. Polymer 2005;46(15):5758–66.
[12] Wang L, Sheng J. Polymer 2005;46(16):6243–9.
[13] Lai SQ, Yue L, Li TS, Liu XJ, Lv RG. Macromol Mater Eng 2005;290:195–201.
[14] Ni P, Li J, Suo J, Li S. J Mater Sci 2004;39(14):4671–3.
[15] Du Z, Rong J, Zhang W, Jing Z, Li H. J Mater Sci 2003;38(24):4863–8.
[16] Rong J, Sheng M, Li H, Ruckenstein E. Polym Compos 2002;23(4):658–65.
[17] Medeiros ES, Tocchetto RS, Carvalho LH, Conceicao MM, Souza AG. J Therm Anal Calorim 2002;67(2):279–85.
[18] Rong J, Jing Z, Li H, Sheng M. Macromol Rapid Commun 2001;22(5):329–34.
[19] Rong J, Li H, Jing Z, Hong X, Sheng M. J Appl Polym Sci 2001;82(8):1829–37.
[20] Wang L, Sheng J. J Macromol Sci, Pure Appl Chem 2003;A40(11):1135–46.
[21] Grandjean J, Bujdak J, Komadel P. Clay Miner 2003;38(3):367–73.
[22] Johnson LM, Pinnavaia TJ. Langmuir 1991;7(11):2636–41.
[23] Okutomo S, Kuroda K, Ogawa M. Appl Clay Sci 1999;15(1–2):253–64.
[24] He J, Shen Y, Yang J, Evans DG, Duan X. Chem Mater 2003;15(20):3894–902.
[25] Fernandez ME, Ascencio JA, Mendoza-Anaya D, Rodriguez Lugo V, Jose-yacaman M. J Mater Sci 1999;34(21):5243–55.
[26] Facey GA, Kuang W, Detellier C. J Phys Chem B 2005;109(47):22359–65.
[27] Kuang W, Facey GA, Detellier C. J Mater Chem 2006;16(2):179–85.
[28] Lan T, Pinnavaia TJ. Chem Mater 1994;6(12):2216–9.